

# Laser-induced Microplasma as Effective Tool for Phase Elements Fabrication on Amorphous and Crystalline Materials

Victoria Shkuratova, Vladimir Rymkevich, Galina Kostyuk, Maksim Sergeev

*ITMO University, 197101, 49, Kronverkskiy av., Saint Petersburg, Russia*  
E-mail: maxim.m.sergeev@gmail.com

Surface precision processing of Iceland spar and fused silica is shown experimentally by laser-induced microplasma action. The optimal regimes allowed to control the relief depth up to  $\sim 14 \mu\text{m}$  with the step of 50 nm are achieved and discussed. Two types of optical elements (random phase plate and spiral phase plate) are fabricated and tested in laser setups, to change initial intensity distribution (Gaussian) to flat-top and annular, consequently. Flap-top distribution characterized by low speckle modulation, i.e. high quality. The annular distribution corresponds to classical concepts.

DOI: 10.2961/jlmn.2018.03.0011

**Keywords:** laser-induced micro plasma, random phase plate, homogenization, flat-top, spiral phase plate, vortex beam, annular laser beam

## 1. Introduction

A lot of attention is paid to the realization of vortex beams with an orbital angular momentum. The field of such beam is characterized by a helicoidal structure of the wave front, where the shape of the intensity distribution (in the far field) corresponds to an annular [1]. The annular beam is in demand in various technological applications [1-3]: laser microprocessing, as an optical tweezer for the manipulation of macroscopic particles, in high-resolution microscopy (to enhance the contrast of phase and amplitude, as well as to increase the resolution of the image formed by the objective) or for cooling and trapping of neutral atoms.

One of the main optical elements (OEs) for realization of optical vortex is a spiral phase plate (SPP). SPP produces a direct transformation of a Gaussian beam into a vortex one without changing the direction of beam propagation [3]. The main material for SPP is a plate of fused silica due to high ray strength and optical transparency in the range of 0.2–4.5  $\mu\text{m}$ .

No less significant attention is paid to the creation of OEs capable of suppressing high-frequency intensity modulation (so-called "hot spots") and transforming the profile of the laser beam in the processing area [4]. One of the main OEs that reduce the contrast of speckles ("hot spots") in the processing area is a random phase plate (RPP) [5]. In this case a multibeam interference of elementary beam is observed. In this context, the laser source with high beam quality ( $M^2 \sim 1.0\text{--}1.2$ ) and the highest degree of coherence is applied [6]. RPP is fabricated on transparent plate (mostly fused silica), where its surface divided on a set of elementary cells, characterized by the equal shape. A half of the cells (drawn at random) are etched to depth  $h = \lambda/2(n - 1)$  [5], where  $n$  – a refraction index of used transparent material,  $\lambda$  – a wavelength of laser source for which the RPP is fabricated. Such a depth is enough to shift

a phase of laser radiation by  $\pi$  that leads to suppression of "hot spots" in the processing area.

Birefringent crystal looks as a promising material for the RPP. The depth of elementary elements should be enough to achieve phase shift by  $\pi$  (according to the expression  $\varphi = 2\pi(n_o - n_e)/\lambda$ , where  $n_o$  is the refraction index of the regular wave and  $n_e$  is the refraction index of the irregular wave. The value  $\Delta = (n_o - n_e)h$  determines the path difference between the ordinary and extraordinary waves arising in the plate. The required phase shift is reached when  $\Delta = (m + 1/2)\lambda$ , where  $m = 0, 1, 2, \dots$  [7]. The etched elementary element (half of the whole set) at the calculated depth rotate the polarization vector of elementary beams by  $90^\circ$  from the initial beam. Since multibeam interference between orthogonal linearly polarized beams is impossible [7], the use of such RPP will provide a significant suppression of the speckle contrast.

It is evident, the fabrication of the RPP have to be on the material obtains the maximum value of the birefringence, that makes it possible to reduce the etching depth and preserve the condition  $\varphi = \pi$ . Iceland spar has the maximum birefringence  $((n_o - n_e) = 0.184$  at  $\lambda = 405 \text{ nm}$ ) of known and available materials (crystal quartz, calcium fluoride etc.) [8] that makes Iceland spar attractive for RPP fabrication. It should be noted, that special laser beams can find various technological applications, for example, in material processing [2], for medical applications [9] and in scientific research [3].

Currently, the main methods of OEs fabrication on glass surface are lithography technology [3] and two-photon direct laser writing [10, 11]. However, considerable attention has recently been paid to the utilize of indirect laser etching methods [5, 12]. Application of laser-induced micro plasma (LIMP) created during explosive type evaporation of absorbing media is the basis for different methods

of transparent materials processing: LIPAA (Laser-Induced Plasma-Assisted Ablation), LIBDE (Laser-Induced Backside Dry Etching), LIBWE (Laser-Induced Backside Wet Etching), LIFE (Laser-Induced Front side Etching), and others [12]. The processed material transparent for laser radiation was positioned in close contact with absorbing target [5] or was placed at some distance from it [13]. In case of close contact the erosion plasma first appeared on the border of absorbing and transparent media due to ablation. This erosion plasma by means of high temperature and pressure created impact on transparent media [14]. Application of massive target with high absorption of laser radiation and low ablation threshold as well as limitation of plasma torch expansion by transparent media of solid plate is the peculiarity of LIMP applied in laser-induced backbody heating (LIBBH) method [15].

This micro plasma is of interest because of high transformation index of laser radiation energy into plasma energy ( $\sim 0.87$ ) which made it effective instrument for transparent media processing [15]. Besides laser processing conditions provided stable control of plasma characteristics and its localization in the space. LIMP properties appearing in LIBBH method differed significantly from that of similar plasma in case of unimpeded divergence implemented for example in LIPAA method [16]. It is known that in the regime of expansion limitation LIMP the luminous intensity of its ion component rises drastically while its lifetime shortens. Utilization of solid massive target and limitation of plasma spreading resulted in significant increase of pressure pulse amplitude on processed material and this contributed to the material etching. As a result, the LIBBH method allowed to increase the efficiency of LIMP application for structuring of transparent material surfaces and also to widen the ability of plasma processing for example for fabrication of OEs [5]. But amorphous glasses differ from crystal materials due to properties anisotropy as well as higher fragility. This makes them more difficult for LIMP etching. Plasma etching of crystal materials often results in their cracking and stratification in processing area as well as accumulation of strain which results in destruction of material after impact [13]. All this reduces control of etching depth and significantly limits fabrication regimen of OEs without defects. Resolving of such problems requires study of LIMP action specifics on amorphous and crystal materials while OEs fabrication methods on such materials become very urgent.

Peculiarities of LIMP application for structuring of amorphous fused silica for creation of spiral phase plate (SPP) as well as Iceland spar with crystal anisotropic structure for creation random phase plate (RPP) were investigated in this work. The results of phase diffraction elements testing are also presented.

## 2. Experiments

Fabrication of SPP on fused silica and RPP on Iceland spar was done by LIBBH method where carbon plasma [15] induced by nanosecond laser pulses of  $1.07 \mu\text{m}$  wavelength was used as instrument for transparent material processing. Yb fiber laser (pulse duration  $\tau = 50 \text{ ns}$ , pulses frequency  $f$  varied from 10 to 100 kHz and average power up to 6 W) was used as radiation source.

The target for plasma initiating was done of solid massive graphite plate with absorption ability of  $A(\lambda = 1.07 \mu\text{m}) \sim 0.95$ . Plates of fused silica or Iceland spar were positioned close to the target and formation of micro relief according to assigned contour which was the template of future OEs took place on them (fig. 1). Movement of erosion plasma torch which etched the transparent material was done along the path of laser beam scanning by means of two mirror galvanometric system. The diameter of laser beam at the two media border was formed by T-Lens with focal lens  $F = 180 \text{ mm}$  and was  $d_0 = 50 \mu\text{m}$  [5].

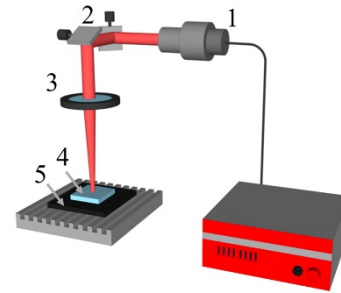


**Fig. 1.** Experimental setup for realization of LIBBH method: 1 – Yb fiber laser, 2 – scanning system, 3 – T-lens, 4 – processed material, 5 – absorbing target

The depth of micro relief formed on fused silica and Iceland spar was measured by contact method on profilometer «Hommel Tester T8000» with resolution in scanning plane  $6 \mu\text{m}$  and depth  $0.01 \mu\text{m}$ . The technological map (depths map) was compiled to coordinate formed micro relief depth and laser processing regime. Visual assessment of processed surface quality was done by means of optical microscopy on «Carl Zeiss Axio Imager». Obtained results were used for the regimen choice of laser action during OE fabrication.

OEs testing was done in two stages: first initial laser beam intensity profile in focal plane of the collective lens was registered then the transformed one by means of SPP and RPP. Registration of intensity change in laser beams section was done using CCD camera Gentec Beamage 3.0 according to schemes on fig. 2.

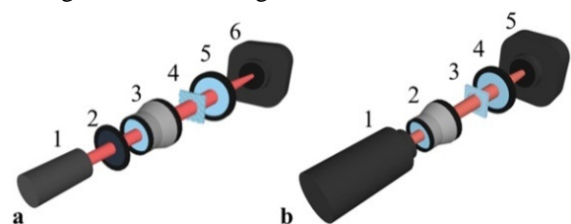


**Fig. 2.** Test diagrams: a) RPP: 1 – laser module ( $\lambda = 405 \text{ nm}$ ), 2 – polarizer, 3 – telescope ( $3^\times$ ), 4 – RPP, 5 – collective lens ( $F = 150 \text{ mm}$ ), 6 – CCD camera; b) SPP: 1 – He-Ne laser ( $\lambda = 633 \text{ nm}$ ), 2 – telescope ( $3^\times$ ), 3 – SPP, 4 – collective lens ( $F = 450 \text{ mm}$ ), 5 – CCD camera

## 3. Materials and Optical Elements

Fused silica and Iceland spar which are usually used for OEs fabrication were selected for investigation of LIBBH action on optical materials. Fused silica was chosen as amorphous material, as noted earlier, since it has highest ray strength compared to other optical glasses. Iceland spar

was used as crystal material which as well as crystal quartz possesses high transmission in optical wavelengths range but its birefringence value in optical wavelengths range exceeds that of crystal quartz almost by 20 times. For example, for  $\lambda = 405 \text{ nm}$   $n_o(\text{SiO}_2) = 1.566$ ,  $n_e(\text{SiO}_2) = 1.557$  and  $n_o(\text{CaCO}_3) = 1.680$ ,  $n_e(\text{CaCO}_3) = 1.496$  [8].

Small value of crystal quartz birefringence required significant depths of its plasma etching for RPP fabrication. For example, the depth of micro relief formed on crystal quartz which facilitates  $90^\circ$  turn of linear polarization vector during radiation passage through etched area should be in the range of  $15\text{--}32 \text{ }\mu\text{m}$  depending on the wavelength. A lot of experiments of LIMP application in LIBBH method show that good control of transparent material etching depth in the range of  $0.05\text{--}3.00 \text{ }\mu\text{m}$  with step  $0.05 \text{ }\mu\text{m}$  which is much less than the etching depth required for OE fabrication on crystal quartz. In case of Iceland spar application the etching depth facilitating condition of polarization vector turn reduced to  $0.9\text{--}2.3 \text{ }\mu\text{m}$  in optical wavelength range and this corresponded to the possible depths range achieved by LIBBH method. It should be mentioned that until now LIMP was not used for structuring of Iceland spar surface in different transparent materials processing methods.

The fabrication of SPP was performed on fused silica. This OE has one flat surface while another one is spiral form (fig. 3). Thickness  $h$  of such plate was varied proportionally to the azimuthal angle  $\varphi$  and was determined by expression [1]:

$$h = s \frac{\varphi}{2\pi} + h_0, \quad (1)$$

where  $s$  – step in height direction,  $h_0$  – base height. Such SPP permitted to transform the Gauss beam into the vortex one with annular distribution of intensity in the far-field without direction change of its propagation [3]. In this case flat wave front incident on SPP transformed into the helicoidal one and phase circulated around the zero amplitude point and created the vortex [1]. The most important stage determining the ability of SPP to create vortex beam was testing based on intensity distribution registration of transformed beam in the far-field.

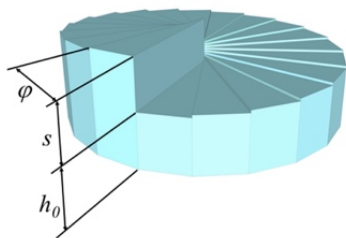


Fig. 3. Schematic image of SPP

The fabrication of RPP (fig. 4). was performed on Iceland spar. The surface of this OE is divided into elementary cells of similar form 50% of which are positioned at random in plate plane and are etched at depth:

$$h = \frac{\lambda}{2(n_o - n_e)}, \quad (2)$$

creating phase shift  $\pi$ , realized at the path difference  $\Delta = (m + 1/2)\lambda$ , where  $m = 0$ .

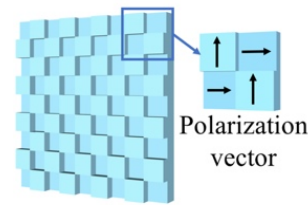


Fig. 4. Schematic image of RPP

#### 4. Mechanism of Etching by LIBBH

The process of micro relief formation by means of transparent material LIBBH etching depends on many factors and does not depend directly on laser beam characteristics. The reason for this is two stage transformation of energy: from laser radiation to plasma and further from plasma to the energy of decomposition and destruction of transparent material. That's why due to the absence of direct analytical relationships between etching depth and laser radiation regimen the depths maps [5] were used for choice of SPP and RPP fabrication regimen.

As a result of depth maps analysis, it was determined that the formation of structures with quality facilitating OEs functioning without cracks and splinters (fig. 5) on fused silica occurred in wide range of average power  $P = 1.1\text{--}5.5 \text{ W}$  at low scanning speeds ( $v = 50\text{--}300 \text{ mm/s}$ ) and pulse frequency following  $f = 20\text{--}80 \text{ kHz}$ . On Iceland spar the relief occurred at significantly lower values of average power  $P = 0.55\text{--}1.10 \text{ W}$  high scanning speeds ( $v = 700\text{--}1000 \text{ mm/s}$ ) and the following pulse frequency following  $f = 50\text{--}80 \text{ kHz}$ . It should mention that LIBBH provides roughness in processing area of  $\sim 50 \text{ nm}$  for both materials.

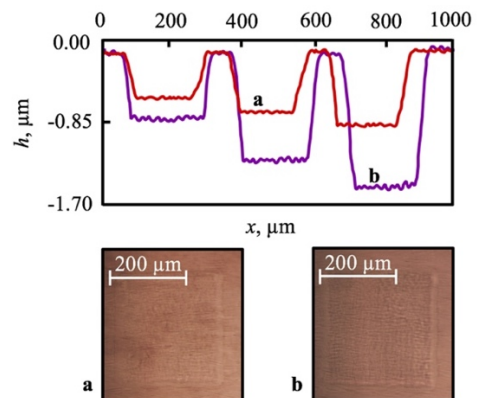


Fig. 5. The micro relief profile of cells: a) fabricated on fused silica at  $f = 50 \text{ kHz}$ ,  $v = 100 \text{ mm/s}$ ,  $P = 3.85\text{--}4.40 \text{ W}$ ; b) fabricated on Iceland spar at  $f = 50 \text{ kHz}$ ,  $v = 800 \text{ mm/s}$ ,  $P = 0.55\text{--}1.1 \text{ W}$

For evaluation of energy contribution in material etching process at required depth  $h$  was chosen energy density in the pulse  $\varepsilon = 4P/\pi d_0^2 f$  which affects laser processing area. The fused silica processing took place at energy density  $\varepsilon = 0.6\text{--}14.0 \text{ J/cm}^2$  for the Iceland spar processing lower  $\varepsilon$  value in the range of  $0.4\text{--}1.1 \text{ J/cm}^2$  was required. Number of pulses  $N = d_0 f/v$  per area of laser action was also evaluated. The ranges of  $N$  for fused silica were  $2\text{--}80$  pulses in case of Iceland spar processing  $N$  reduced to  $3\text{--}6$  pulses. During one scan the depth of etched cells in fused silica varied from  $0.03$  to  $1.18 \text{ }\mu\text{m}$  in Iceland spar it was from  $0.5$  to  $1.3 \text{ }\mu\text{m}$ . The increase of Iceland spar etching depth can

be achieved by 5 or 10 scans in sequence in existing range  $\varepsilon$  since increase of energy density resulted in material destruction. As a result, etching depth of Iceland spar after 5 scans increased to 8  $\mu\text{m}$  and reached 14  $\mu\text{m}$  after 10 scans. With increase of scans number the pulses number in the area of laser action reached  $N = 60$ . For visual comparison of fused silica and Iceland spar processing conditions by LIBBH method the graphs of formed micro relief depth depending on such laser radiation parameters as energy density and number of laser pulses are presented on fig. 6.

The differences of laser processing regimen are due to fragility of used materials. The hardness of Iceland spar which is more fragile was 3 on Moos scale, for fused silica the hardness on Moos scale was 7. Due to this for processing of Iceland spar energy density and pulses number in the area of laser action were reduced and required etching depth was achieved by increase of scans number.

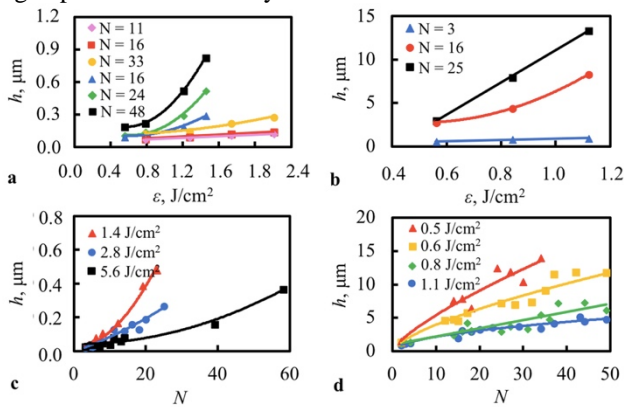


Fig. 6. Dependence formed micro relief depth on energy density and number of laser pulses for: a, c) fused silica; b, d) Iceland spar

### 5. Fabrication and Testing of SPP and RPP

Values of etching depth  $h$  of each of SPP sectors (fig. 7 a) facilitating phase shift of incident on it radiation with wavelength  $\lambda$  in the range from 0 to  $2\pi$  were calculated according to the relationship [3]:

$$h = \frac{(m-1)\lambda}{m_{\max}(n-1)}, \quad (3)$$

where  $n$  – refraction index of SPP material,  $m = 1, 2, \dots, m_{\max}$  – sector number,  $m_{\max} = 20$ . In case of RPP fabrication (fig. 7 b) etching depth  $h$  of elementary cells of square form ( $250 \times 250 \mu\text{m}$ ) which creates incident radiation phase shift  $\pi$  and polarization vector turn  $90^\circ$  was calculated according to the expression (2).

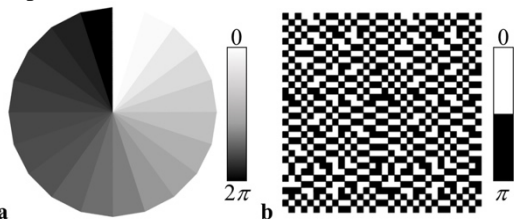


Fig. 7. Templates for OEs fabrication: a) SPP; b) RPP

Based on experimental results the regimen were chosen of laser radiation appropriate for SPP and RPP fabrication and ensuring best surface quality of these OEs (table 1).

Table 1 Regimen of SPP (on fused silica,  $n = 1.46$ ) and RPP (on Iceland spar,  $n_o = 1.680, n_e = 1.496$ ) fabrication

	$\lambda$ , nm (n)	$h$ , $\mu\text{m}$	$P$ , W	$f$ , kHz	$v$ , mm/s	Scans
SPP	633	0÷1.315	4÷18	40	50÷300	1
RPP	405	1.12	3	70	700	1

After fabrication OEs were tested in optical setups presented on fig. 2. The profile of initial radiation beam from laser module with wavelength  $\lambda = 405 \text{ nm}$  formed in the focal plane of collective lens had intensity distribution of Gauss beam (fig. 8a). After positioning of RPP before the collective lens the intensity distribution profile in its focal plane within the limits of central diffraction maximum acquired flat-top (fig. 8b). It is important to note that interference pattern contrast (pattern of speckles) in the central part of the profile facilitated by interference of elementary laser beams from each RPP cell was significantly reduced due to the turn of laser radiation polarization vector which passed through etched cells. Profile of He-Ne laser of  $\lambda = 633 \text{ nm}$  wavelength and mode  $\text{TEM}_{00}$  intensity distribution in the collective lens focal plane also had Gauss form (fig. 8 c). After insertion of SPP into the optical scheme the Gauss beam transformed into the annular one (fig. 8d) and this confirmed functionality of fabricated SPP.

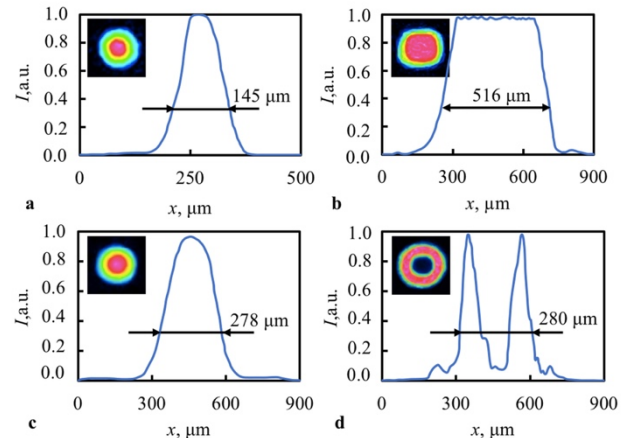


Fig. 8. Test results: a) initial laser beam for RPP testing, b) laser beam after RPP; c) initial laser beam for SPP testing, d) laser beam after SPP

Initial beams diameters generated by laser module ( $\lambda = 405 \text{ nm}$ ,  $M^2 \sim 5.8$ ) and by He-Ne laser ( $\lambda = 633 \text{ nm}$ ,  $M^2 = 1.1$ ) in collective lens focal plane were evaluated experimentally (fig. 8 a, c) and according to the expression [17]:

$$d_f = \frac{4M^2 \lambda F}{D_L}, \quad (4)$$

where  $M^2$  – beam quality factor,  $F$  – collective lens focal length,  $D_L$  – beam diameter in the collective lens location plane. The  $d_f$  values for laser module and He-Ne laser were equal to  $140 \mu\text{m}$  and  $278 \mu\text{m}$  respectively. Beam diameter in collective lens focal plane for the RPP positioned in optical scheme was evaluated using expression [4]:

$$d = \frac{2\lambda F}{d_{el}}. \quad (5)$$

It was 486  $\mu\text{m}$  for elementary cell RPP  $d_{el} = 250 \mu\text{m}$ .

The homogenization quality calculated using expression [6]:

$$C = \frac{\sigma}{\langle I \rangle}, \quad (6)$$

where  $\sigma$  – standard intensity deviation,  $\langle I \rangle$  – average intensity value.  $C$  value was  $\sim 1.3\%$ , and this confirmed significant reduction of intensity modulation when RPP is used.

In case of SPP application external diameter of annular distribution of intensity formed in collective lens focal plane was evaluated according to intensity level of  $1/e^2$  times and appeared to be 280  $\mu\text{m}$ . All results of estimating calculations in all cases showed satisfactory coincidence with experimental results.

## 6. Conclusion

The possibility of Iceland spar utilization with high value of birefringence  $n_o - n_e$  ( $\lambda = 405 \text{ nm}$ ) = 0.184 as crystal material for fabrication RPP by LIBBH method was demonstrated in this work. Peculiarities of Iceland spar surface plasma etching which differ from processing conditions of amorphous fused silica were investigated. It was found that on Iceland spar which is more fragile compared to amorphous fused silica less energy density  $\varepsilon = 0.4\text{--}1.1 \text{ J/cm}^2$  and lesser pulse number in the area of laser action that is  $N = 3\text{--}6$  compared to fused silica should be used. It was also found that on Iceland spar it is possible to increase etching depth up to 14  $\mu\text{m}$  by means of several scans in sequence (5–10) with energy density  $\varepsilon = 0.4\text{--}1.1 \text{ J/cm}^2$ .

OEs that is SPP on fused silica and RPP on Iceland spar were fabricated by means of LIBBH. After fabrication of OEs both types were tested in appropriate optical schemes. The tests confirmed effectiveness of SPP functioning which allowed to obtain annular beam with external diameter 280  $\mu\text{m}$ . Quality of beam homogenization after fabricated RPP was  $\sim 1.3\%$ .

## Acknowledgments

The reported study was financially supported by the Ministry of Education and Science of the Russian Federation, research agreement № 14.587.21.0037 (RFMEFI58717X0037).

## References

- [1] S.S.R. Oemrawsingh, J.A.W. Van Houwelingen, E.R. Eliel, J.P. Woerdman, E.J.K. Verstegen and J.G. Kloosterboer: *Appl. Opt.*, 43, (2004) 688.
- [2] M. Duocastella and C.B. Arnold: *Laser Photon. Rev.*, 6, (2012) 607.
- [3] C. Jun, K. Deng-Feng, G. Min and F. Zhi-Liang: *Chin. Phys. Lett.*, 26, (2009) 014202.
- [4] S.N. Dixit, I.M. Thomas, B.W. Woods, A.J. Morgan, M.A. Hennesian, P.J. Wegner and H.T. Powell: *Appl. Opt.*, 32, (1993) 2543.
- [5] R. Zakoldaev, G. Kostyuk, V. Rymkevich, V. Koval, M. Sergeev, V. Veiko, E. Yakovlev and A. Sivers: *J. Laser Micro/Nanoengin.*, 12, (2017) 281.

- [6] Z. Deng, Q. Yang, F. Chen, H. Bian, J. Yong, G. Du, Y. Hu and X. Hou: *IEEE Photon. Tech. Lett.*, 26, (2014) 2086.
- [7] M. Born and E. Wolf: "Principles of optics: electromagnetic theory of propagation, interference and diffraction of light", (Elsevier, Oxford, 2013) p.790.
- [8] D.S. Kliger and J.W. Lewis: "Polarized light in optics and spectroscopy", (Academic Press, Boston, 2012) p.39.
- [9] D. Serien and K. Sugioka: *Opto-Electron. Adv.*, 1, (2018) 180008.
- [10] T. Gissibl, S. Thiele, A. Herkommer and H. Giessen: *Nat. Photon.*, 10, (2016) 554.
- [11] Y. Li, L. Chen, F. Kong, Z. Wang, M. Dao, C. T. Lim, F. Li and M. Hong: *Opto-Electron. Eng.*, 44, (2017) 393.
- [12] Y. Hanada, K. Sugioka, Y. Gomi, H. Yamaoka, O. Otsuki, I. Miyamoto and K. Midorikawa: *Appl. Phys. A*, 79, (2004) 1001.
- [13] Y. Hanada, K. Sugioka, I. Miyamoto and K. Midorikawa: *Appl. Surf. Sci.*, 248, (2005) 276-280.
- [14] B. Hopp, T. Smausz, T. Csizmadia, C. Vass, T. Csako and G. Szabo: *J. Laser Micro/Nanoengin.*, 5, (2010) 80.
- [15] V.P. Veiko, S.A. Volkov, R.A. Zakoldaev, M.M. Sergeev, A.A. Samokhvalov, G.K. Kostyuk and K.A. Milyaev: *Quant. Electron.*, 47, (2017) 842.
- [16] S. Xu, B. Liu, C. Pan, L. Ren, B. Tang, Q. Hu and L. Jiang: *J. of Mater. Proc. Tech.*, 247, (2017) 204.
- [17] W.M. Steen and J. Mazumder: "Laser material processing", (Springer-Verlag London Limited, London, 2010) p.102.

(Received: June 28, 2018, Accepted: October 13, 2018)